CDK5 targets p21^{CIP1} to regulate thyroid cancer cell proliferation and malignancy in patients

MIN-CHE TUNG[1], MUHAMMET ONER[2], SHIUAN-WOEI SOONG[2,3], PANG-TING CHENG[2], YU-HSUAN LI[2,3], MEI-CHIH CHEN[3], CHEN-KAI CHOU[4], HONG-YO KANG[5-7], FRANK CHEAU-FENG LIN[8,9], STELLA CHIN-SHAW TSAI[10-12] and HO LIN[2]

[1]Department of Surgery, Tungs' Taichung MetroHarbor Hospital, Taichung 43503, Taiwan, R.O.C.; [2]Department of Life Sciences, National Chung Hsing University, Taichung 40227, Taiwan, R.O.C.; [3]Translational Cell Therapy Center, Department of Medical Research, China Medical University Hospital, Taichung 40447, Taiwan, R.O.C.; [4]Division of Endocrinology and Metabolism, Department of Internal Medicine, Kaohsiung Chang Gung Memorial Hospital, College of Medicine, Chang Gung University, Kaohsiung 833, Taiwan, R.O.C.; [5]Graduate Institute of Clinical Medical Sciences, Chang Gung University College of Medicine, Taoyuan 83301, Taiwan, R.O.C.; [6]Department of Biological Science, National Sun Yat-sen University, Kaohsiung 804959, Taiwan, R.O.C.; [7]Center for Hormone and Reproductive Medicine Research, Department of Obstetrics and Gynecology, Kaohsiung Chang Gung Memorial Hospital, Chang Gung University, College of Medicine, Kaohsiung 83301, Taiwan, R.O.C.; [8]School of Medicine, Chung Shan Medical University, Taichung 402367, Taiwan, R.O.C.; [9]Department of Surgery, Chung Shan University Hospital, Taichung 402367, Taiwan, R.O.C.; [10]Department of Otolaryngology, Tungs' Taichung MetroHarbor Hospital, Taichung 43503, Taiwan, R.O.C.; [11]College of Life Sciences, National Chung Hsing University, Taichung 40227, Taiwan, R.O.C.; [12]Department of Post-Baccalaureate Medicine, National Chung Hsing University, Taichung 40227, Taiwan, R.O.C.

Received October 21, 2024; Accepted March 12, 2025

DOI: 10.3892/mmr.2025.13547

Abstract. Cyclin-dependent kinase 5 (CDK5), known for its role in neuronal function, has emerged as a key player in cancer biology, particularly in thyroid cancer. The present study explored the interaction between CDK5 and the cyclin-dependent kinase inhibitor p21^{CIP1} in thyroid cancer (TC). Bioinformatic tools and immunoprecipitation assays were used to confirm that CDK5 targets p21 for ubiquitin-mediated degradation, reducing its stability and tumor-suppressive effects. Data from The Cancer Genome Atlas revealed a significant inverse correlation between CDK5 and p21 expression, with higher CDK5 levels linked to increased tumor malignancy and worse survival outcomes; conversely, higher p21 expression was correlated with an improved prognosis. Immunohistochemistry analysis of TC samples further confirmed that increased CDK5 and reduced p21 expression were associated with more advanced tumor stages and aggressive phenotypes. These findings suggested that CDK5-mediated degradation of p21 contributes to TC progression and malignancy, highlighting the potential of targeting the CDK5-p21 axis as a therapeutic strategy for management of TC.

Correspondence to: Professor Ho Lin, Department of Life Sciences, National Chung Hsing University, 145 Xingda Road, Taichung 40227, Taiwan, R.O.C.
E-mail: hlin@dragon.nchu.edu.tw

Dr Stella Chin-Shaw Tsai, College of Life Sciences, National Chung Hsing University, 145 Xingda Road, Taichung 40227, Taiwan, R.O.C.
E-mail: tsaistella111@nchu.edu.tw

Key words: papillary thyroid cancer, malignancy, cell proliferation, cyclin-dependent kinase 5, cyclin-dependent kinase inhibitor 1

Introduction

Cyclin-dependent kinase 5 (CDK5) is a serine/threonine kinase that, unlike other members of the CDK family, is not directly involved in cell cycle regulation (1). Instead, CDK5 plays a crucial role in various neuronal processes including brain development, synaptic plasticity and neuronal migration (2-4). Dysregulation of CDK5 activity has been linked to several neurodegenerative disorders, highlighting its significance in maintaining neural integrity and function. Studies have also begun to elucidate the involvement of CDK5 in non-neuronal tissues and its emerging role in cancer biology (1,5,6). CDK5 is activated by binding to its neuron-specific activators, p35 and p39, which are essential for its kinase activity. In the context of cancer, aberrant activation of CDK5 has been implicated in promoting tumor progression and metastasis in various types of cancer, influencing cellular processes such as migration, invasion and angiogenesis, highlighting it as a potential target for therapeutic intervention in cancer cells (1,6-15).

p21$^{CIP1/WAF1}$, commonly referred to as p21, is a critical regulator of the cell cycle, known for its role as a CDK inhibitor (16). Encoded by the CDKN1A gene, p21 primarily functions by binding to and inhibiting the activity of cyclin-CDK2 or

-CDK4 complexes, thus playing a pivotal role in the G_1 phase of the cell cycle (17). This inhibition prevents the phosphorylation of the retinoblastoma protein, effectively halting cell cycle progression and allowing the cell time to repair DNA damage or, if necessary, initiate apoptosis (18,19). p21 is tightly regulated by the tumor suppressor protein p53, which induces p21 expression in response to DNA damage and other stress signals (16,20,21). Through this mechanism, p21 acts as a safeguard against uncontrolled cell proliferation, making it a key player in maintaining genomic stability and preventing tumorigenesis (22). Beyond its role in the cell cycle, p21 is also involved in several other cellular processes, including apoptosis, transcriptional regulation and cell senescence (16). The dual role of p21 in both cell cycle arrest and the promotion of cell survival makes it a complex and context-dependent factor in cancer biology. While the function of p21 as a tumor suppressor is well-established, its role in cancer can be paradoxical. In certain contexts, particularly when p53 is mutated, p21 can contribute to tumor progression by promoting cell survival and resistance to chemotherapy (23). Understanding the multifaceted roles of p21 in cancer, particularly its interactions with other cellular proteins such as CDK5, is crucial for developing targeted therapies that exploit these pathways for cancer treatment.

Thyroid cancer (TC) is a malignancy that originates in the thyroid gland, a small, butterfly-shaped organ located at the base of the neck (24). The thyroid gland plays a crucial role in regulating the body's metabolism through the production of hormones such as thyroxine and triiodothyronine (25). Although TC is relatively uncommon compared with other types of cancer, it is the most prevalent endocrine malignancy and its incidence has been increasing globally over the past few decades (26,27). There are several distinct types of TC, each with unique characteristics and prognoses. The most common form is papillary (P)TC, which accounts for ~80% of all TC cases (28,29). PTC generally has a favorable prognosis, with high survival rates, especially when detected early (30). However, a subset of PTC cases can be aggressive, leading to local invasion, recurrence and distant metastasis (31-34). Other types of TC include follicular TC (35), medullary TC (36) and the most aggressive form, anaplastic TC (37), which is rare but highly lethal. TC is often diagnosed through the detection of a thyroid nodule, followed by further evaluation with ultrasound, fine-needle aspiration biopsy and molecular testing (38). Treatment typically involves surgical removal of the thyroid gland (thyroidectomy) (39), followed by radioactive iodine therapy in certain cases (40). While several patients respond well to these treatments, a subset with aggressive disease or metastatic spread may require additional therapies, including targeted therapies or external beam radiation (41). Research into the molecular mechanisms underlying TC has revealed a variety of genetic and environmental factors that contribute to its development. Mutations in genes such as BRAF, RAS and RET/PTC are commonly implicated in TC (6,42), while alterations in the PI3K/AKT and MAPK signaling pathways are frequently observed in more aggressive forms of the disease (43-45). Understanding these molecular drivers has led to the development of targeted therapies aimed at inhibiting these pathways, offering new hope for patients with advanced TC. Despite advances in diagnosis and treatment, challenges remain in managing aggressive and recurrent TC cases. Continued research is essential to identify novel therapeutic targets and improve outcomes for patients with this complex and increasingly common disease.

In the present study, the biochemical interaction between CDK5 and p21 in PTC cells was assessed and the functional consequences of this interaction on cell proliferation and malignancy were explored. Using advanced bioinformatic tools such as AlphaFold 3.0 and Chimera X for protein-protein interaction analysis alongside immunoprecipitation (IP) assays, it was shown that CDK5 targeted p21 for ubiquitin-dependent degradation. Furthermore, the findings were validated using clinical tumor samples and data from The Cancer Genome Atlas (TCGA), highlighting the clinical relevance of CDK5 and p21 in TC. The results not only elucidated a novel regulatory mechanism involving CDK5 and p21 but also suggested potential therapeutic strategies targeting this pathway to curb TC progression. Given the emerging role of CDK5 in cancer, these findings open novel avenues for research and development of CDK5 inhibitors as anti-cancer agents.

Materials and methods

Ethical approval. The present study was approved by the Institutional Review Board of Tungs' Taichung MetroHarbor Hospital, Taichung, Taiwan. (approval no. 113003). All experimental procedures followed the relevant ethical guidelines and informed consent was obtained from all patients with TC included in the present study. Thyroid tissue samples were collected from a cohort of these patients.

Patient samples. The patient samples were collected from Tungs' Taichung MetroHarbor Hospital, Taichung Taiwan. Samples were collected between 2024/05/01 and 2024/05/31. A total of 11 patients participated in the study, five samples for each patient, and a total of 55 samples were collected for analysis. Samples were preserved and processed for immunohistochemical (IHC) analysis to evaluate the expression of specific proteins. Clinical data on the patients' age, sex and cancer staging were obtained from the hospital's electronic medical records (Table I). All samples were anonymized to ensure patient confidentiality in accordance with Institutional Review Board (IRB) regulations.

IHC staining. The expression of proteins was assessed using IHC on formalin-fixed, paraffin-embedded tissue sections. The sections were cut into 4 μm thick slices and mounted on positively charged glass slides. The slides were deparaffinized in xylene and rehydrated using a decreasing series of graded alcohol solutions, followed by a rinse in distilled water. For antigen retrieval, heat-induced epitope retrieval using a citrate buffer (pH 6.0) was performed for 20 min in a pressure cooker. To block endogenous peroxidase activity, sections were incubated with 3% hydrogen peroxide (H_2O_2) in methanol for 10 min at room temperature, followed by washing in PBS. After retrieval, the slides were allowed to cool to room temperature and then washed in PBS. To block non-specific binding, the slides were incubated with 5% normal goat serum (Vector Laboratories, Inc. cat. no. ZH083) with blocking solution for 30 min at room

Table I. Patients background and IHC profile.

Patient	Age, years	Sex	Cancer stage	TNM staging	Malignancy features	IHC profile	Expression profile (%)
Patient 1	62	Male	I	T1a, Nx, Mx	None	Moderate CDK5, Moderate p21	~57
Patient 2	60	Male	II	T1b, N1b, Mx	None	High CDK5, Low p21	~65
Patient 3	61	Male	III	T4a, N0, Mx	Recurrence	High CDK5, Low p21	~70
Patient 4	54	Male	I	T1a, Nx, Mx	Double Cancer	High CDK5, Low p21	~55
Patient 5	42	Female	I	T1a, N0, Mx	None	Moderate CDK5, High p21	~46
Patient 6	32	Female	I	T1b, Nx, Mx	None	Moderate CDK5, Moderate p21	~60
Patient 7	24	Female	I	T1b, N0, Mx	None	Moderate CDK5, Moderate p21	~57
Patient 8	70	Female	I	T2, N0, Mx	None	Moderate CDK5, Moderate p21	~58
Patient 9	63	Female	IVA	T1b, N1b, Mx	Recurrence	High CDK5, low p21	~95
Patient 10	58	Female	II	T2, N1, Mx	None	Moderate CDK5, Moderate p21	~58
Patient 11	48	Female	I	T1a, Nx, Mx	None	Moderate CDK5, Moderate p21	~50

IHC, immunohistochemistry; CDK5, cyclin-dependent kinase.

temperature. The tissue sections were incubated overnight at 4˚C with the following primary antibodies: Mouse monoclonal anti-CDK5 (cat. no. sc-249; Santa Cruz Biotechnology, Inc.; 1:20) or rabbit polyclonal anti-p21 (cat. no. 2947; Cell Signaling Technology, Inc.; 1:50). After washing the slides in PBS, they were incubated with appropriate biotinylated secondary antibodies for 30 min at room temperature (Goat anti-mouse IgG, cat. no. BA-9200 or Goat anti-rabbit IgG, cat. no. BA-1000; Vector Laboratories, Inc.; dilution 1:200), followed by a wash in PBS. Signals were visualized using a horseradish peroxidase (HRP)-conjugated streptavidin detection system (Vectastain ABC kit, Vector Laboratories, Inc.). The slides were developed using 3,3'-diaminobenzidine (DAB; Dako) as the chromogen for 5 min at room temperature and counterstained with hematoxylin to visualize nuclei for 2 min at room temperature. Finally, the sections were dehydrated, cleared in xylene and a coverslip was placed over them using a permanent mounting medium. Positive control slides were included for each staining run. Negative controls were performed by omitting the primary antibodies to assess non-specific binding of the secondary antibody.

Imaging and analysis. Stained slides were scanned using a high-resolution digital microscope (Zeiss Imager. Z2; Carl Zeiss AG) and images were captured for analysis. Protein expression was semi-quantitatively evaluated based on staining intensity and the percentage of positive cells using TissueFAXS viewer version 7.1.6. supplied by TissueGnostics GmbH. The results were classified into low, moderate, or high expression levels. Statistical analysis was performed to evaluate the correlation between protein expression and clinical outcomes in patients with TC.

Cell culture and transfection. Human TC cell lines BCPAP and TPC-1 were purchased from the Food Industry Research and Development Institute in Taiwan. The two TC cell lines were provided by collaborators Dr Chen-Kai Chou and Dr Hong-Yo Kang in Kaohsiung Chang Gung Hospital (Taiwan) (46). Cells were maintained in RPMI-1640 culture medium (Gibco; Thermo Fisher Scientific, Inc.), supplemented with 10% FBS (Gibco; Thermo Fisher Scientific, Inc.), penicillin-streptomycin at concentrations of 100 IU/ml and 100 μg/ml, respectively (MilliporeSigma), along with 2 mM L-glutamine, 1.5 g/l sodium bicarbonate ($NaHCO_3$) (MilliporeSigma), 10 mM HEPES (MilliporeSigma) and 1 mM sodium pyruvate (MilliporeSigma). For cell transfection, cells were transfected with either short hairpin (sh)RNA targeting CDK5 (shCDK5) or a scrambled shRNA control (shCtrl) using Lipofectamine® 2000 (Invitrogen; Thermo Fisher Scientific, Inc.) as the transfection reagent for 6 h at 37˚C. Overexpression plasmids were transfected in the same manner. Transfections were performed in serum-free medium according to the manufacturer's protocol. After 6 h of incubation, the transfection medium was replaced with fresh complete medium and cells were cultured for an additional 24-48 h before proceeding with downstream analyses. Plasmids used for transfection were obtained

from the National RNAi Core Facility (Academia Sinica). Specifically, the pLKO.1 plasmid harboring shRNA sequence targeting CDK5 or scrambled control (shCtrl) were used at a concentration of 2 μg/ml. The target sequences of shGFP and shCDK5 were: TRCN0000072192 (shGFP): 5'-GAACGG CATCAAGGTGAACTT-3', TRCN0000021466 (shcdk5 #1): 5'-TGTCCAGCGTATCTCAGCAGA-3', TRCN0000199652 (shcdk5 #2): 5'-GTGAACGTCGTGCCCAAACTC-3', TRCN0000194974 (shcdk5 #3): 5'-CCTGAGATTGTAAAG TCATTC-3'.

Reverse transcription-quantitative (RT-q) PCR. Total RNA was extracted from cultured cells using TRIzol reagent (Invitrogen; Thermo Fisher Scientific, Inc.) following the manufacturer's instructions. RNA quality and concentration were assessed by spectrophotometry. Reverse transcription was performed using 1 μg of total RNA with the High-Capacity cDNA Reverse Transcription Kit (Applied Biosystems; Thermo Fisher Scientific, Inc.) according to the manufacturer's instructions. qPCR was performed using SYBR Green (Roche Applied Science) on a real-time PCR system by using Applied Biosystems StepOnePlus (Applied Biosystems; Thermo Fisher Scientific, Inc.) as described previously (22). Gene expression levels were normalized to the housekeeping gene, and relative quantification was calculated using the $2^{-\Delta\Delta Cq}$ method as described previously by Livak and Schmittgen (47). The thermocycling conditions were as follows: initial denaturation at 95˚C for 10 min, followed by 40 cycles of denaturation at 95˚C for 15 sec, annealing and extension at 60˚C for 1 min. Each experiment was performed in triplicate and independently replicated at least three times. The following primers were used to amplify the cDNA: CDKN1A (5'-ACCCTAGTTCTACCTCAGGC-3' and 5'-AAGATCTAC TCCCCCATCAT-3'), CDK5 (5'-TCTTTTTCCCGGCAATGA T-3' and 5'-TCTGGCAGCTTGGTCATAGA-3'), and actin (5'-TTGCCGACAGGATGCAGAA-3' and 5'-GCCGATCCA CACGGAGTACT-3').

Western blotting. Cells were lysed at approximately 80-90% confluency using lysis buffer [50 mM Tris-HCl (pH 7.4), 150 mM NaCl, 1% NP-40, 0.5% sodium deoxycholate, 0.1% SDS] supplemented with a protease inhibitor cocktail (MilliporeSigma). Protein concentrations were measured using a BCA Protein Assay Kit (Pierce; Thermo Fisher Scientific, Inc.). Equal amounts of protein (30 μg per lane) were separated by electrophoresis on 10% SDS-polyacrylamide gels (SDS-PAGE) and transferred onto polyvinylidene fluoride (PVDF) membranes (MilliporeSigma). Membranes were blocked in 5% non-fat dry milk (MilliporeSigma) in TBS containing 0.1% Tween-20 (TBST) for 1 h at room temperature. After blocking, membranes were incubated overnight at 4˚C with primary antibodies diluted in blocking buffer: anti-CDK5 (cat. no. ab40773; Abcam; 1:1,000) and anti-p21 (cat. no. 2947; Cell Signaling Technology, Inc.; 1:1,000). After incubation, membranes were washed three times (5 min each) in TBST (Tris-buffered saline containing 0.1% Tween-20). Subsequently, membranes were incubated with HRP-conjugated secondary antibodies (goat anti-rabbit IgG-HRP, cat. no. 7074, 1:5,000; goat anti-mouse IgG-HRP, cat. no. 7076, 1:5,000; Cell Signaling Technology, Inc.) at room temperature for 1 h. Following incubation, membranes were washed three times (5 min each) in TBST. Proteins were visualized using enhanced chemiluminescence (ECL) detection reagent (Pierce ECL Western Blotting Substrate; Thermo Fisher Scientific, Inc.) according to the manufacturer's protocol. Signal intensities were captured using a chemiluminescent imaging system (Bio-Rad Laboratories, Inc.). β-actin (cat. no. 4970; Cell Signaling Technology, Inc.; dilution 1:2,000) was used as the loading control. Each experiment was independently repeated at least three times.

IP. IP was performed as previously described (48). Briefly, BCPAP and TPC-1 cells were seeded into 10-cm culture dishes at a density of ~$1x10^6$ cells per dish and cultured until reaching 80-90% confluency. BCPAP and TPC-1 cells were lysed in IP lysis buffer (50 mM Tris-HCl pH 7.5, 150 mM NaCl, 1 mM EDTA, 1% NP-40 and protease inhibitors). Protein concentration was determined using a BCA Protein Assay Kit (Pierce; Thermo Fisher Scientific, Inc.). Equal amounts of protein lysate (500 μg) were incubated with 2 μg anti-CDK5 antibody (Abcam) overnight at 4˚C with gentle rotation. Protein A/G agarose beads (Thermo Fisher Scientific, Inc.) were added and incubated for an additional 2 h at 4˚C. Input controls (30 μg of total protein lysate without immunoprecipitation) were included for western blot analysis to confirm the presence of target proteins. Beads were washed three times with ice-cold washing buffer (20 mM Tris-HCl pH 7.4, 150 mM NaCl, 0.1% NP-40) and proteins were eluted with SDS sample buffer by boiling for 5 min. Eluates were analyzed using 10% SDS-PAGE followed by western blotting using an anti-p21 antibody (cat. no. 2947; Cell Signaling Technology, Inc.) as aforementioned.

Protein stability assay and MG132 treatment. Protein stability assays were performed as previously described (49). To assess p21 protein stability, BCPAP and TPC-1 cells were treated with cycloheximide (CHX; MilliporeSigma) at a final concentration of 50 μg/ml to inhibit protein synthesis. Cells were collected at 0, 2, 4 and 6 h post-CHX treatment. For proteasome inhibition, cells were treated with 10 μM MG132 (Calbiochem; Merck KGaA) for 6 h prior to lysis. Cell lysates were prepared and protein levels of p21 and CDK5 were determined by western blotting as aforementioned. β-Actin (Cell Signaling Technology, Inc.) was used as the loading control.

Immunocytochemistry. Immunocytochemistry was performed as previously described (3). Briefly, cells were fixed for 5 min in 4% paraformaldehyde and 2% sucrose in PBS at room temperature. Subsequently, the cells were permeabilized and blocked in PBS buffer containing 0.1% Triton X-100 and 5% bovine serum albumin (Cyrus Bioscience, Lot no. 1260601) for 15 min at room temperature. The primary antibodies CDK5 (Santa Cruz Biotechnology, Inc.; cat. no. sc-249; dilution 1:100) and p21 (Cell Signaling Technology, Inc.; cat. no. 2947; dilution 1:200) were diluted in 5% BSA in PBS and added to the cells for overnight incubation at 4˚C. Then, the cells were incubated with Alexa Fluor 488-conjugated secondary antibodies (Thermo Fisher Scientific, Inc.; cat. no. A-11008; dilution 1:1,000) and Alexa Fluor 546-conjugated secondary antibodies (Thermo Fisher Scientific, Inc.; cat. no. A-11003;

dilution 1:1,000) for 1 h at room temperature. The cells were washed again with PBS and counterstained with DAPI (Thermo Fisher Scientific, Inc.) for 5 min at room temperature. Cells were subsequently washed with PBS, mounted using Fluoromount-G (Southern Biotech; cat. no. 0100-01) and analyzed using a fluorescence microscope (Olympus BX-51; Olympus Corporation) and a Zeiss LSM510 confocal microscope (Carl Zeiss AG).

Bioinformatics analysis for protein-protein interactions. The 3D structures of proteins were visualized as previously described (3). The interaction between CDK5 and p21 was predicted using AlphaFold 3.0, an AI-based protein structure prediction tool (50). The protein structures were visualized and analyzed for interaction sites using UCSF Chimera software (Resource for Biocomputing, Visualization, and Informatics, University of California, San Francisco, CA, USA). Chimera was used to map potential interaction interfaces and validate the predicted binding sites.

TCGA data analysis. TCGA data analysis was performed as previously reported (5). Expression data and clinical information for patients with TC were downloaded from TCGA using the UCSC Xena browser (https://xenabrowser.net/). Pearson correlation analysis was performed to evaluate the relationship between CDK5 and p21 mRNA expression levels. Kaplan-Meier survival analysis was conducted using the 'survival' package in R to compare overall survival between high and low-expression groups for CDK5 and p21. Kaplan-Meier survival analysis was performed using the 'survival' package in R. Differential expression analysis between tumor and normal tissues was assessed using the Wilcoxon rank-sum test. Violin plots were generated to visualize the stage-specific expression of CDK5 and p21 across different stages of TC. Differential expression analysis was conducted to compare CDK5 and p21 expression in tumor compared with normal tissues, with statistical significance assessed using the Wilcoxon rank-sum test. Statistical analyses and visualizations, including Pearson correlation, Kaplan-Meier survival analysis, violin plots, and differential expression analysis, were conducted using R software (R Core Team, 2023). R: A language and environment for statistical computing. R Foundation for Statistical Computing, Vienna, Austria (http://www.R-project.org/).

Statistical analysis. All statistical analyses were conducted using GraphPad Prism version 8.0.1 (Dotmatics). Data are presented as the mean ± SD of at least three independent experiments. Comparisons between two groups were performed using an unpaired Student's t-test. Pathological stage plots were obtained from GEPIA (http://gepia.cancer-pku.cn/), and differential gene expression was analyzed by one-way ANOVA followed by Tukey's post hoc test. $P<0.05$ was considered to indicate a statistically significant difference.

Results

CDK5 interacts with p21. The interaction between CDK5 and $p21^{CIP1}$ is pivotal for understanding the regulatory mechanisms underlying cell cycle progression and tumor suppression in TC. To investigate this interaction, AlphaFold 3.0, a cutting-edge AI-based protein structure prediction tool, was used to generate a model of the CDK5-p21 protein-protein interaction. The accuracy of AlphaFold in predicting protein structures based on amino acid sequences provided a reliable foundation for the analysis (50). Using data generated from AlphaFold, Chimera was used to visualize and analyze the interaction sites between CDK5 and p21. The analysis revealed that CDK5 directly interacted with specific regions of the p21 protein, indicating potential sites for regulation through phosphorylation and other post-translational modifications (Fig. 1A-D). This interaction is significant as it implies modulation of the stability of p21 and activity in TC cells, potentially contributing to enhanced cell proliferation and malignancy. To experimentally validate the CDK5-p21 interaction, IP assays were performed using the TC cell line TPC-1. Additionally, cells were treated with MG132, a proteasome inhibitor, to prevent proteasomal degradation and ensure the detection of any ubiquitin-dependent degradation products. The IP analysis confirmed that CDK5 biochemically interacted with p21 protein in TPC-1 cells, reinforcing the computational predictions and suggesting a direct regulatory relationship between CDK5 and p21 in TC (Fig. 1D). These findings provide a comprehensive understanding of the CDK5-p21 interaction, demonstrating its potential role in modulating cell cycle regulation and promoting the malignancy of TC.

CDK5 reduces p21 protein stability and induces TC cell proliferation. To investigate the role of CDK5 in the regulation of $p21^{CIP1}$ in TC cells, several experiments were performed to analyze protein interactions, degradation and cellular localization. TC cells transfected with either an empty vector (EV) or CDK5 were treated with CHX to inhibit protein synthesis. Western blot analysis showed that p21 levels decreased more rapidly in cells overexpressing CDK5 compared with the EV control. This suggested that CDK5 accelerated p21 degradation (Fig. 2A and B). Next, cells were treated with MG132, a proteasome inhibitor, to block protein degradation. In mock-treated cells, overexpression of CDK5 resulted in lower p21 levels compared with the EV control. In MG132-treated cells, p21 levels did not differ markedly between CDK5-overexpressing cells and EV controls. In addition, IHC was used to further confirm the results. In control cells (vector), p21 was normally expressed, while in CDK5-overexpressing cells, p21 levels were visibly reduced. Upon MG132 treatment, p21 levels were restored in CDK5-overexpressing cells, confirming the role of proteasome-mediated degradation (Fig. 2C-E). The data collectively demonstrate that CDK5 downregulates p21 in TC cells by promoting its ubiquitin-dependent degradation via the proteasome pathway. This regulatory mechanism suggests a significant role for CDK5 in modulating cell cycle progression and tumor development in TC by targeting p21 for degradation. To further elucidate the mechanism by which CDK5 regulated p21, Co-IP experiments were performed to analyze the interaction between CDK5 and p21. Wild-type (WT) p21 and its phosphorylation-deficient mutant (MT; S130A) were compared. Western blot analysis revealed that CDK5 effectively interacted with WT, as shown by the co-precipitation of CDK5 and p21 proteins (Fig. 2F). However, the intensity of the interaction signal was lower for

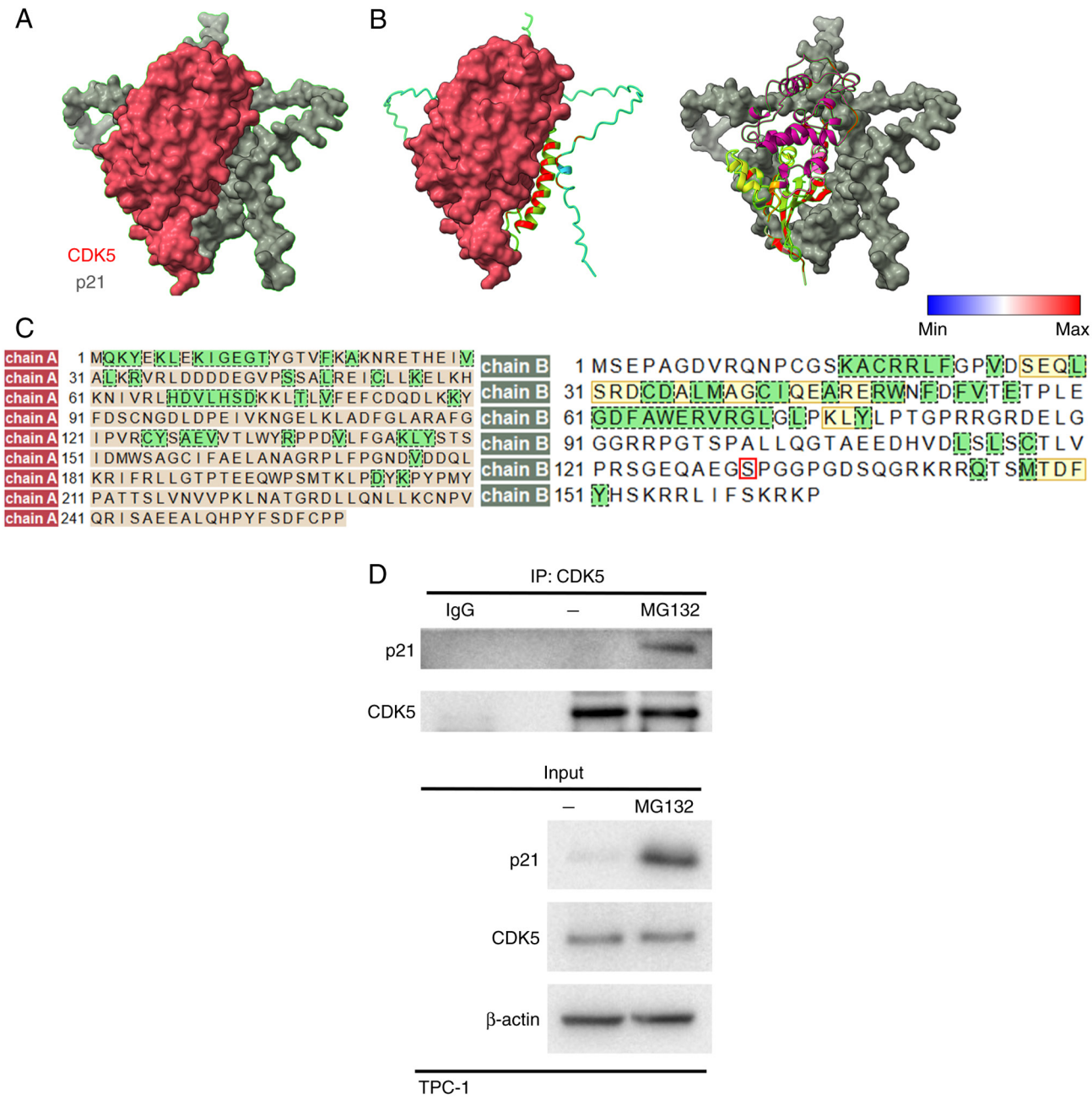

Figure 1. CDK5 interacts with p21. (A) Structural prediction of the interaction between CDK5 and p21 using AlphaFold 3.0. CDK5 is shown in red and p21 in green. (B) Detailed visualization of the CDK5-p21 interaction interface using UCSF Chimera software. CDK5 is shown in surface representation, while p21 is depicted in a ribbon diagram. The binding sites are highlighted. Heat map of the interaction interface indicating the degree of interaction strength between CDK5 and p21, with red representing strong interaction sites and blue representing weak or no interaction. (C) Sequence alignment of CDK5 and p21 showing the interacting regions predicted by AlphaFold. Residues involved in the interaction are highlighted in red for CDK5 and green for p21. (D) Immunoprecipitation assay demonstrating the interaction between CDK5 and p21 in TPC-1 cells. Cells were treated with 10 μM MG132 to inhibit proteasomal degradation. CDK5 was immunoprecipitated from cell lysates and co-precipitated p21 was detected by western blotting. Input lysates (bottom panels) show the expression levels of p21, CDK5 and β-actin, the latter was used as the loading control. The results confirm the interaction between CDK5 and p21 and suggested that CDK5 regulates p21 stability via the ubiquitin-proteasome pathway. CDK5, cyclin-dependent kinase 5.

MT p21, suggesting that the S130 site influenced the strength of the CDK5-p21 interaction (Fig. 2F). To assess the functional impact of CDK5-mediated p21 regulation on cell proliferation, TC cells were analyzed for their proliferation rates in the presence of WT and MT p21. The results showed that CDK5 overexpression markedly enhanced cell proliferation when WT p21 was present. By contrast, cells expressing MT p21 (S130A) displayed suppressed CDK5-mediated proliferation (Fig. 2G), suggesting that the phosphorylation of p21 at the S130 site is essential for CDK5 to promote cell proliferation. These findings indicated that the phosphorylation-deficient mutant p21 (S130A) blocks the ability of CDK5 to enhance cell proliferation, thereby acting as a dominant-negative form to counteract CDK5-mediated oncogenic effects. The data collectively suggested that CDK5 promoted cell proliferation in TC by targeting p21 for phosphorylation-dependent degradation and that MT p21 can serve as a potential therapeutic tool to inhibit CDK5-driven tumor progression.

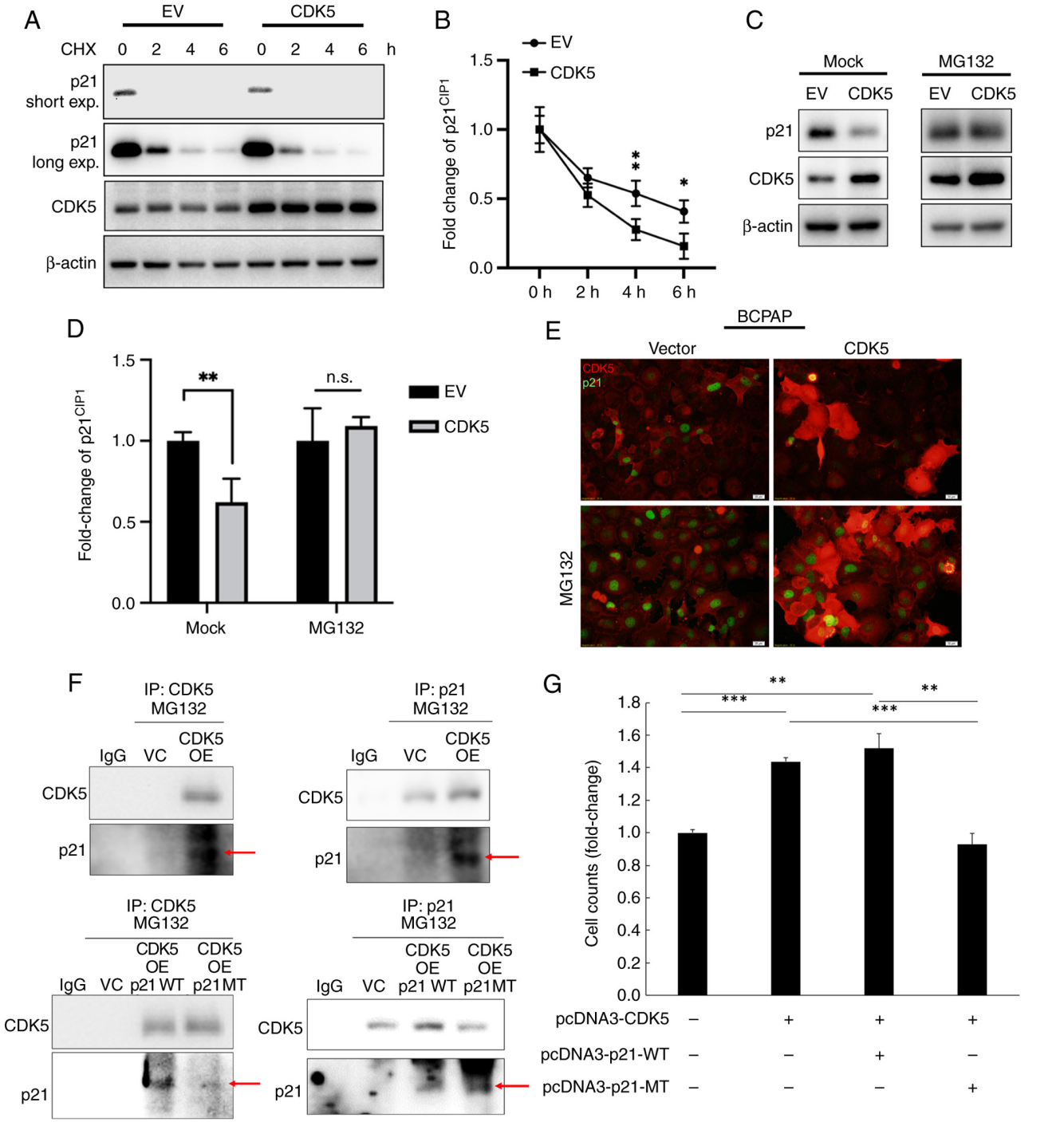

Figure 2. CDK5 downregulates p21 in TC cells. (A) Western blot analysis of p21 protein expression levels in BCPAP cells transfected with EV or a CDK5 overexpression plasmid. Cells were treated with 50 μg/ml CHX for 0, 2, 4 or 6 h to inhibit protein synthesis. Short and long exposures of p21 are shown. (B) Quantification of p21 protein levels. Data are presented as the fold change relative to time 0 for EV and CDK5 transfected cells. (C) Western blot analysis of p21 and CDK5 protein expression levels in BCPAP cells transfected with EV or CDK5, with or without treatment with 10 μM MG132 for 6 h. (D) Quantification of p21 protein expression. Data are presented as fold change relative to EV-transfected mock-treated cells. (E) Immunofluorescence staining of p21 (green) in BCPAP cells transfected with vector or CDK5, with or without MG132 treatment. The results indicate that CDK5 overexpression reduces p21 levels in TC cells and this effect was reversed following proteasome inhibition. Scale bar, 20 μm. (F) Co-immunoprecipitation analysis of CDK5 and p21 was performed to investigate the interaction between CDK5 and p21 in thyroid cancer cells. Panels show the interaction of CDK5 with WT p21 and MT p21 following proteasome inhibition using MG132. Red arrows indicate the presence of p21 in the immunoprecipitated complex. (G) Cell counting assay was performed to evaluate p21 WT and MT p21 on cell proliferation. For all blots, β-actin was used as the loading control. Values are presented as the mean ± SD from three independent experiments. Data were compared using an unpaired Student's t-test. *P<0.05, **P<0.01, ***P<0.001. CDK5, cyclin-dependent kinase; 5TC, thyroid cancer; EV, empty vector; HCX, cycloheximide; n.s., not significant; WT, wild-type; MT, S130A mutant.

CDK5 negatively regulates p21 expression in TC cells. To further elucidate the regulatory relationship between CDK5 and p21^{CIP1} in TC cells, several experiments examining mRNA and protein expression levels, as well as the effects of CDK5 knockdown were performed. RT-qPCR was used to measure the mRNA expression levels of CDK5 in BCPAP

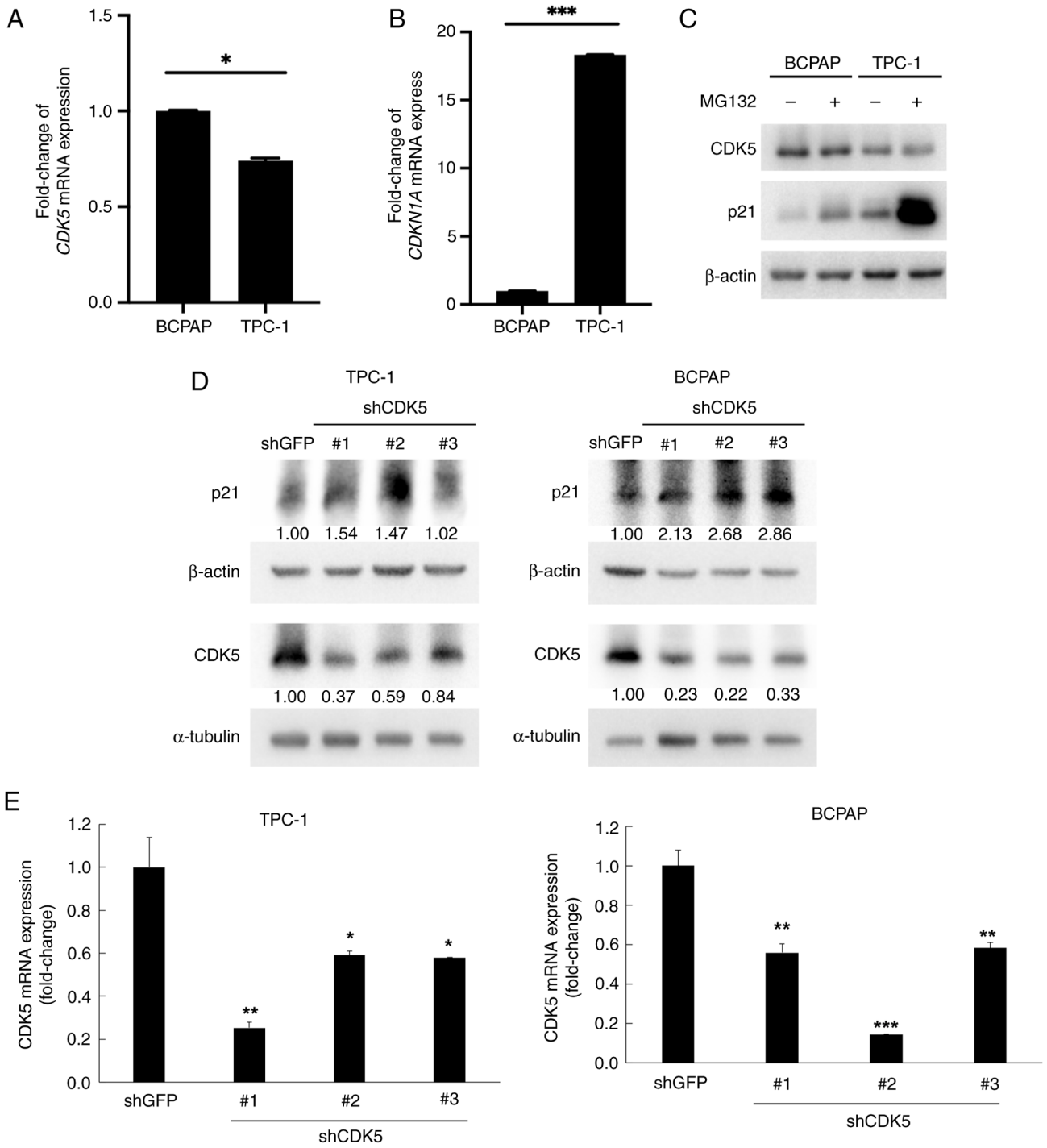

Figure 3. CDK5 negatively regulates p21 in TC cells. Reverse transcription-quantitative PCR analysis of (A) CDK5 and (B) CDKN1A mRNA expression in TC cell lines BCPAP and TPC-1. (C) Western blot analysis of p21 and CDK5 protein levels in BCPAP and TPC-1 cells treated with or without 10 μM MG132 for 6 h. (D) Western blot analysis of p21 and CDK5 protein levels in TPC-1 and BCPAP cells transfected with shGFP or shCDK5 (#1, #2, and #3). (E) Quantitative analysis of CDK5 mRNA levels in both TPC-1 and BCPAP cells. Data are presented as the fold change relative to shGFP-transduced cells. The results demonstrated that knockdown of CDK5 increases p21 protein expression levels in TC cells. Values are presented as the mean ± SD from three independent experiments. Data were compared using an unpaired Student's t-test. *P<0.05, **P<0.01, ***P<0.001 vs. shGFP. CDK5, cyclin-dependent kinase; TC, papillary thyroid cancer; sh, short hairpin; n.s., not significant.

and TPC-1 cells. The results showed markedly higher CDK5 mRNA expression in BCPAP cells compared with TPC-1 cells (Fig. 3A). In addition, TPC-1 cells had markedly higher p21 mRNA expression levels than BCPAP cells (Fig. 3B). Western blot analysis was performed to examine the protein expression levels of CDK5 and p21 in BCPAP and TPC-1 cells, both with and without MG132 treatment. In the absence of MG132, TPC-1 cells showed higher levels of CDK5 and lower levels of p21 expression compared with BCPAP cells. MG132 treatment increased p21 levels in both cell lines, but the increase was more pronounced in TPC-1 cells, indicating that CDK5 promoted p21 degradation through the proteasome pathway (Fig. 3C). In addition, TPC-1 and BCPAP cells were transfected with shRNAs targeting CDK5 (shCDK5 #1,

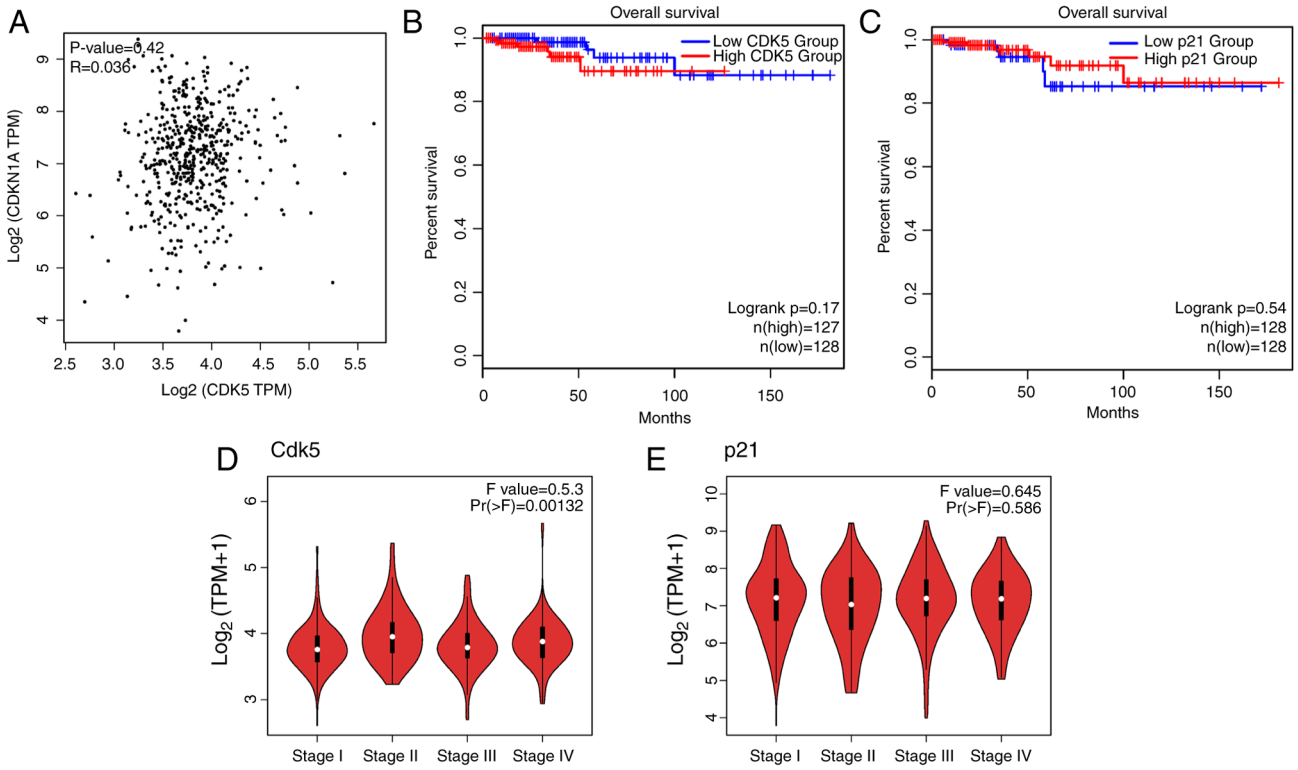

Figure 4. Analysis of TCGA data showing the clinical relevance of CDK5 and p21 in thyroid cancer. (A) Scatter plot showing the correlation between CDK5 and p21 mRNA expression in thyroid cancer samples from TCGA. Pearson correlation coefficient (r) and P-value are indicated. (B) Kaplan-Meier overall survival analysis of patients with thyroid cancer stratified by high and low CDK5 expression levels. (C) Kaplan-Meier overall survival analysis of patients with thyroid cancer stratified by high and low p21 expression levels. Survival was compared using a log-rank test. (D) Pathological stage plot showing CDK5 expression levels across different stages of thyroid cancer. (E) Pathological stage plot illustrating p21 expression levels across different stages of thyroid cancer. Pathological stage plots were obtained from GEPIA, and differential gene expression was analyzed by one-way ANOVA (https://gepia.cancer-pku.cn/). Higher CDK5 expression was associated with poorer overall survival, while p21 expression was not markedly associated with survival outcomes. TCGA, The Cancer Genome Atlas; CDK5, cyclin-dependent kinase.

shCDK5 #2 and shCDK5 #3) or a control shRNA (shGFP). Following CDK5 knockdown, p21 protein expression levels were measured. Cells with CDK5 expression knocked down exhibited a significant increase in p21 levels compared with the shGFP control (Fig. 3D and E). This indicated that CDK5 negatively regulates p21 expression, as knockdown of CDK5 led to an increase in p21 protein expression levels.

CDK5 contributes to tumor malignancy in patients with TC. To understand the clinical relevance of CDK5 and $p21^{CIP1}$ expression in TC, data from TCGA were analyzed. The analysis included correlation, survival, stage-specific expression and differential expression between tumor and normal tissues. A scatter plot showing the correlation between CDK5 and p21 mRNA expression levels in TC samples is shown in Fig. 4. The correlation coefficient (R) was 0.42, with a P-value <0.03, indicating a significant correlation between CDK5 and p21 expression in TC tissues (Fig. 4A). In addition, patients with high CDK5 expression had worse overall survival compared with those with low CDK5 expression (Fig. 4B). Conversely, patients with high p21 expression tended to have improved overall survival (Fig. 4C), indicating a negative correlation between CDK5 and p21 expression. Violin plots were used to show the expression levels of CDK5 and p21 across different stages of TC. CDK5 expression increases with advancing cancer stage, showing a difference between early-stage (Stage I/II) and late-stage cancer (Stage III/IV) (Fig. 4D). However, p21 expression decreased with advancing cancer stage, with a difference between early and late stages (Fig. 4E). Analysis of data from TCGA revealed a significant negative correlation between CDK5 and p21 expression in TC, supporting the experimental findings that CDK5 negatively regulated p21. Survival analysis indicated that high CDK5 expression was associated with poorer overall survival, while high p21 expression tended to be linked with improved survival outcomes. Additionally, CDK5 expression increased and p21 expression decreased with advancing cancer stage, suggesting their roles in TC progression. Differential expression analysis confirmed that CDK5 was up-regulated and p21 was down-regulated in TC tissues compared with normal tissues. These findings underscore the clinical relevance of targeting the CDK5-p21 axis in TC treatment.

CDK5 and p21 expression in TC specimens are correlated with tumor aggressiveness. IHC staining was performed to assess CDK5 and p21 expression in TC specimens from 11 patients (Fig. 5A). The expression profiles were analyzed in relation to tumor stage, sex and malignancy features (TNM staging; Table I and Data S1). In all cases, CDK5 and p21 were localized to the nuclei and cytoplasm of tumor cells. A distinct pattern emerged where patients with more advanced TNM stages, lymph node involvement, or recurrent tumors exhibited higher

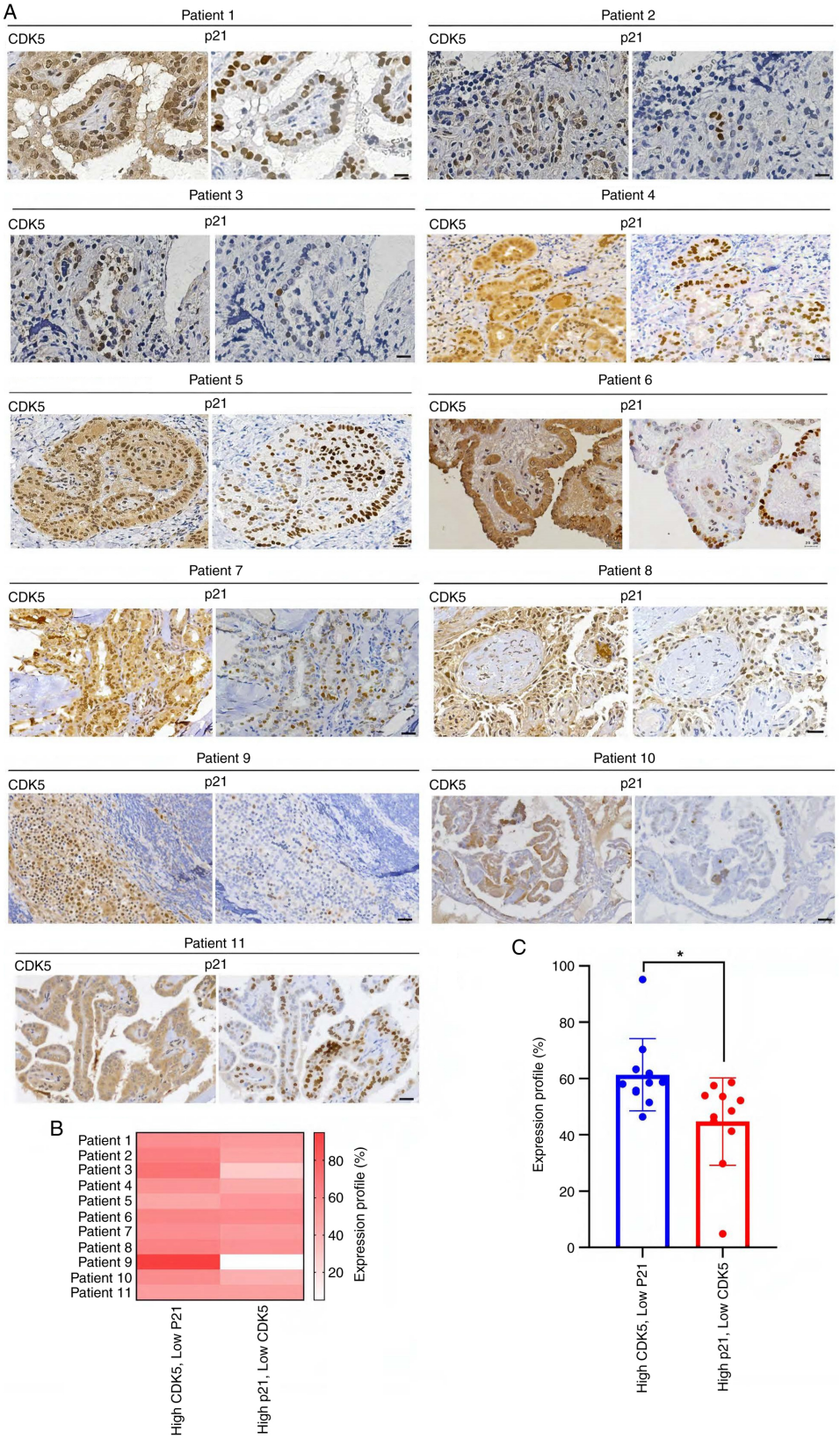

Figure 5. IHC analysis of CDK5 and p21 nuclear expression in papillary thyroid cancer patient specimens. (A) IHC staining for CDK5 and p21 in patients with thyroid cancer demonstrating the relationship between CDK5 and p21 nuclear expression. Left panels, CDK5 staining showed strong nuclear localization in several patient samples, particularly in tumor cells. The nuclear expression of CDK5 was more prominent in aggressive regions of the thyroid cancer samples, suggesting a role in tumor proliferation. Right panels, p21 staining was inversely correlated with CDK5. In samples where CDK5 was strongly expressed in the nucleus, p21 nuclear staining was weak or absent. Conversely, in areas were CDK5 expression was low, p21 nuclear localization was more evident. This expression pattern supported the hypothesis that CDK5 negatively regulated p21 expression at the nuclear level, contributing to cancer cell cycle dysregulation and malignancy. Scale bar, 50 μm. (B) The heatmap illustrates the correlation between nuclear CDK5 and p21 expression across multiple samples, with darker red indicating higher CDK5 expression and lower p21 levels. (C) Significant differences in expression patterns between groups with high CDK5/low p21 and low CDK5/high p21 expression (*P<0.05). This suggested that elevated nuclear CDK5 was associated with decreased p21 expression, supporting the hypothesis that CDK5 promoted thyroid cancer progression. IHC, immunohistochemistry; CDK5, cyclin-dependent kinase.

CDK5 and lower p21 expression (Fig. 5 and Table I). Notably, high CDK5 expression, particularly in patients 2, 3 and 9, was associated with more advanced-stage cancer (II, III and IVA) and malignancy features such as recurrence and invasion into surrounding structures. By contrast, moderate CDK5 and p21 expression were predominantly observed in early-stage cancers (Stage I), such as in patients 1, 6, 7, 8 and 11, where tumors remained smaller and confined to the thyroid. Notably, high p21 expression, as seen in patient 5, was rare and may suggest the presence of a unique tumor suppression pathway (Fig. 5A, Table I and Data S1). A comparative analysis of protein expression revealed that patients with more advanced cancer had a predominance of high CDK5 and low p21 expression, particularly in those with nodal involvement or invasive features, while early-stage patients had higher expression levels of p21 relative to CDK5 (Fig. 5B and C). These observations suggest a potential role of CDK5 in promoting tumor progression and a tumor-suppressive function for p21, with differential CDK5 and p21 expression profiles (Fig. 5), serving as valuable indicators for assessing tumor progression and identifying high-risk patients.

Discussion

The results of the present study provided novel insights into the role of CDK5 and p21 in the progression and malignancy of human TC. The interaction between CDK5 and p21 was shown to play a critical role in cell cycle regulation, impacting the proliferation of cancer cells and consequently, the progression of TC.

TC is the most prevalent type of thyroid malignancy, representing ~80% of all TC cases (51,52). Despite its generally favorable prognosis, characterized by slow growth and a high survival rate, a significant subset of patients presents with aggressive disease (53). These aggressive forms are marked by recurrence, resistance to treatment and distant metastases, which substantially worsen patient outcomes (54-56). Understanding the molecular mechanisms driving TC progression is vital for developing more effective therapies.

CDK5, a serine/threonine kinase, is known for its role in neuronal development and function (2-4). However, its aberrant activity has been increasingly linked to various types of cancer, where it influences critical processes such as cell migration, invasion and metastasis (57-59). CDK5 exerts these effects by interacting with various cellular proteins, including those involved in cell cycle regulation (22,60,61). p21, a well-established cyclin-dependent kinase inhibitor, serves as a crucial tumor suppressor by inhibiting cell cycle progression and thereby preventing uncontrolled cell proliferation (22). The degradation of p21 can lead to the loss of cell cycle control, fostering an environment conducive to tumor growth and malignancy (22,62). In the context of TC, the interaction between CDK5 and p21 has not been explored, to the best of the authors' knowledge. Considering the role of CDK5 in other types of cancer and the findings of the present study, which show its interaction with p21 across various cancer types (22), it was hypothesized that CDK5 may interact with p21 to regulate TC cell proliferation, potentially contributing to the malignancy of TC.

The results of the present study demonstrated that CDK5 interacted with p21, specifically targeting the phosphorylation site at S130 and facilitated its ubiquitin-dependent degradation in TC cells. The regulation of p21 degradation is a highly orchestrated process involving specific ubiquitin chain types and recognition domains, which are critical for its proteasomal targeting (63). The K48-linked polyubiquitin chains are the primary signals for p21 degradation, facilitated by domains such as the PIP box and KRR motif that enable interactions with key E3 ubiquitin ligases (63). In TC, dysregulation of these mechanisms may enhance p21 degradation, contributing to unchecked proliferation and tumor progression. Upstream regulatory factors, particularly those influencing CDK5 activation, such as its co-activators p35 and p39 and oncogenic signaling pathways such as PI3K/AKT and MAPK, probably modulate the interaction between CDK5 and p21 (64). These pathways may influence CDK5 activity through post-translational modifications, including phosphorylation of CDK5 or p21, altering their binding affinity and promoting p21 destabilization (22,63,65). Furthermore, additional molecular partners may facilitate p21 ubiquitination in TC; for example, PCNA acts as a scaffold for $CRL4^{Cdt2}$-mediated p21 ubiquitination during replication stress, while E3 ligases such as MDM2 play similar roles in other cellular contexts (66). The involvement of deubiquitinates such as USP7 or USP10 further complicates the regulation by counteracting ubiquitin-dependent degradation, stabilizing p21 under certain conditions. These molecular interactions create a finely tuned balance of p21 levels, where aberrant regulation can favor tumor progression. Exploring these pathways in TC provides critical insights into the mechanisms underlying p21 degradation and CDK5 activity, offering potential therapeutic opportunities to stabilize p21, restore cell cycle regulation and inhibit CDK5-driven oncogenic processes (Fig. 6). Therefore, advanced bioinformatic tools, such as AlphaFold 3.0 (50,67) were used to predict and analyze the protein-protein interaction between CDK5 and p21. These predictions were experimentally validated using IP assays, which confirmed the biochemical interaction between CDK5 and p21 in TC cells. Additionally, analysis of clinical data from TCGA revealed a significant negative correlation between CDK5 and p21 expression levels in TC tissues. High CDK5 expression was associated with poor overall survival, while high p21 expression was correlated with improved survival outcomes. This suggested that CDK5 contributes to TC progression by potentially promoting the degradation of p21, thereby enabling uncontrolled cell proliferation and disrupting cell cycle regulation (Fig. 6).

In addition, the present study presented evidence linking the expression of CDK5 and p21 to TC progression, with specific correlations to tumor aggressiveness, TNM stage, sex and age from clinical specimens. Based on the data presented in Fig. 5, several hypotheses can be discussed regarding these findings. The results of the immunohistochemistry analysis suggested a clear association between the expression of CDK5/p21 and tumor stage. Patients with higher TNM stages, lymph node metastasis, or recurrence (such as Patients 2 and 3) demonstrated high CDK5 and low p21 expression. In these patients, CDK5 may be contributing to the enhanced tumor invasiveness and metastatic potential, while the reduced expression of p21, an inhibitor of cell cycle progression, could be facilitating unchecked cellular proliferation. This observation supported the hypothesis that CDK5 functions as an oncogene in TC,

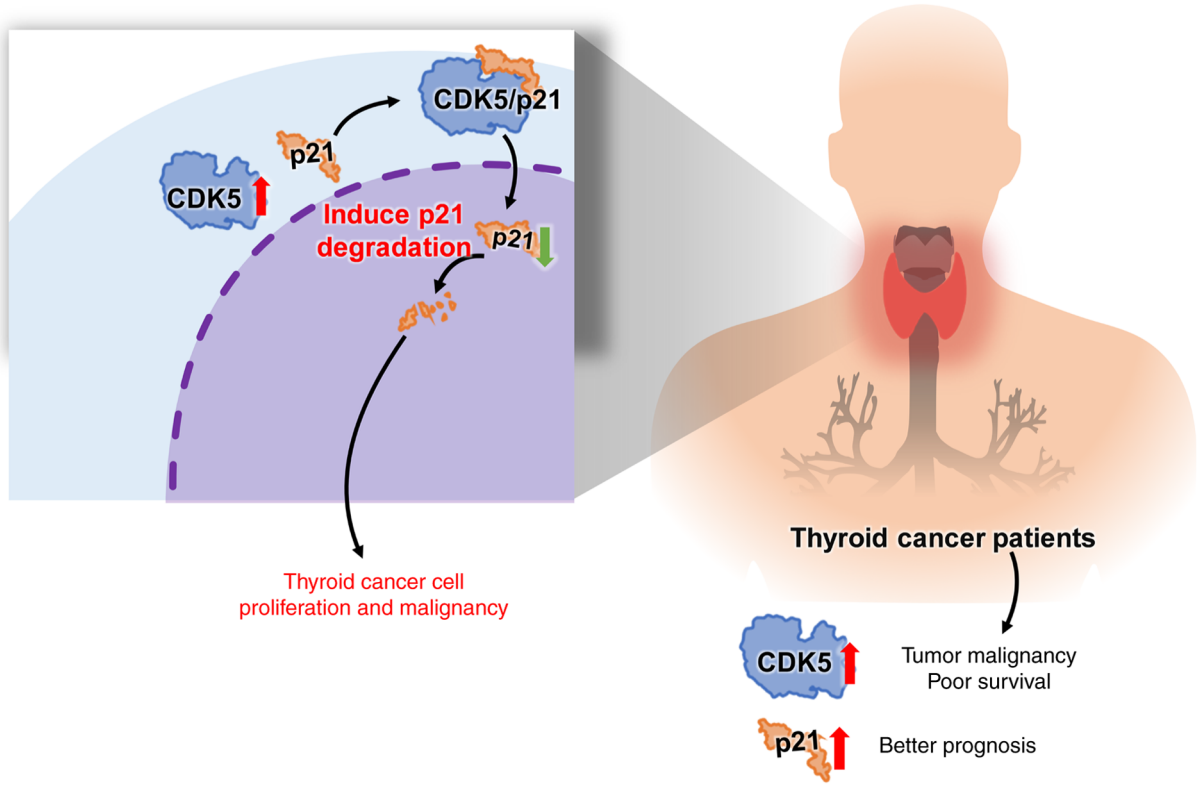

Figure 6. Graphical abstract. The present study examined the interaction between CDK5 and the cyclin-dependent kinase inhibitor p21[CIP1]. CDK5 promoted the degradation of p21 through the ubiquitin-mediated pathways, thereby reducing the tumor-suppressive effects of p21. High CDK5 levels were associated with increased tumor malignancy and worse survival outcomes, while higher p21 expression was associated with an improved prognosis. TC stages and aggressive tumors exhibit elevated CDK5 and reduced p21 levels. This suggested that CDK5-mediated degradation of p21 contributed to TC progression. CDK5, cyclin-dependent kinase 5; TC, thyroid cancer.

promoting malignancy, while p21 acts as a tumor suppressor. Patients with higher CDK5 expression, particularly those with advanced TNM staging, lymph node involvement, or recurrence, exhibited more aggressive tumor characteristics. These findings suggested that CDK5 promoted tumor progression, invasion and metastasis, making it a potential therapeutic target for aggressive TCs. Reduced p21 expression in more advanced cases of cancer (such as Patients 2, 3, 9 and 10) may lead to uncontrolled cell growth, contributing to tumor invasion and metastasis. These results highlighted the importance of p21 in maintaining tumor suppressive activity. This supported the hypothesis that an imbalance between CDK5 and p21 may be linked to cancer recurrence and the development of secondary malignancies. In summary, the findings suggested that CDK5 and p21 played crucial roles in TC progression. High CDK5 expression correlated with aggressive tumor features, while high p21 expression was associated with early-stage, less invasive cancers. These observations provide a basis for further investigation into the roles of CDK5 and p21 as potential therapeutic targets or prognostic biomarkers in TC, with implications for patient stratification and treatment.

In the present study, how CDK5 could serve as a novel therapeutic target in TC by targeting p21 through degradation and altering tumor progression was shown. The observed variability in p21 expression levels across different stages of TC suggested its potential as a biomarker along with CDK5 expression status as another biomarker for disease progression and treatment response, enabling improved stratification of patients based on their tumor biology. Furthermore, the interplay between CDK5 expression/activation and p21 stability highlighted the need for future studies to evaluate small molecule inhibitors that specifically target CDK5 or its upstream regulators to inhibit CDK5 activation or prevent CDK5-p21 interaction (22,65,68,69). This approach could be particularly beneficial in the subset of patients with TC with aggressive disease, where current treatments are less effective. Future research should focus on developing small molecule inhibitors of CDK5 or exploring gene therapy approaches to downregulate CDK5 expression in TC cells (70). These strategies could be tested in preclinical models to evaluate their efficacy in halting TC progression. Additionally, combining CDK5 inhibitors with existing therapies could potentially enhance treatment outcomes (71-74), offering a novel avenue for improving the prognosis of patients with advanced TC. However, while the present study provided valuable insights into the role of the CDK5-p21 axis in TC, there are certain limitations to consider. First, the findings were based on *in vitro* experiments, which, although useful for understanding molecular mechanisms, might not fully reflect the complexity of the tumor microenvironment or systemic factors observed in clinical settings. Second, the study lacked animal experiments, which are crucial for validating the *in vitro* findings and understanding the physiological and pathological relevance of the CDK5-p21 axis *in vivo*. Third, while the analysis included 11 patient cases, the sample size was relatively small, which may limit the broader applicability of the findings. Finally, the

detailed molecular mechanisms underlying CDK5-mediated p21 ubiquitination, including the involvement of specific E3 ubiquitin ligases and regulatory pathways, remain to be fully clarified and warrant further investigation, although the CDK5-p21 interaction was identified in the present study. Despite these limitations, the results laid a strong foundation for future studies to further validate these findings in more complex models and larger patient cohorts.

In conclusion, this study distinguished itself by examining the role of CDK5 in regulating p21 via phosphorylation at the S130 site, a relatively unexplored mechanism in TC. This specific phosphorylation event introduces an additional regulatory layer that markedly affects the stability and function of p21, which has not been adequately addressed in TC. The results of the present study highlighted the critical role of the CDK5-p21 interaction in TC and highlighted novel diagnostic and therapeutic targets that could be exploited to improve patient outcomes. Further exploration of CDK5 inhibitors in clinical settings may pave the way for more effective treatments of this common yet often aggressive cancer.

Acknowledgements

Not applicable.

Funding

The present study was supported by the National Science and Technology Council, Taiwan (grant nos. 109-2320-B-005-004-MY3, 109-2911-I-005-003 and 112-2320-B-005-008 to H. Lin); joint grant of Taichung Veterans General Hospital and National Chung Hsing University (grant no. TCVGH-NCHU1117614 to H. Lin). Tungs' Taichung MetroHarbor Hospital Grant (grant nos. TTMHH-R1120062 and TTMHH-R1130044) and Tungs' Taichung MetroHarbor Hospital and National Chung Hsing University Grant (grant no. TTMHH-NCHULS112004) in Taiwan.

Availability of data and materials

The data generated in the present study may be requested from the corresponding authors.

Authors' contributions

MO, ST and HL contributed to the conception and design of the study. MT, MO, SS and PC were responsible for data acquisition. MO, SS, PC, YL, CC, HK, FL and MC analyzed and interpreted the data. MT, MO, CC, HK, FL, ST, and HL drafted the manuscript and revised it critically for important intellectual content. ST and HL provided supervision and confirm the authenticity of all the raw data. All authors read and approved the final manuscript.

Ethics approval and consent to participate

The present study was conducted with the approval of the Institutional Review Board (IRB) under protocol number 113003. All experimental procedures followed ethical guidelines, and informed consent was obtained from all TC patients involved in this study. Thyroid tissue samples were collected from a cohort of TC patients. The samples were preserved and processed for IHC analysis to evaluate the expression of specific proteins. Clinical data on patients' age, sex, and cancer staging were obtained from the hospital's electronic medical records. All samples were anonymized to ensure patient confidentiality in accordance with IRB regulations.

Patient consent for publication

Not applicable.

Competing interests

The authors declare that they have no competing interests.

References

1. Oner M, Lin E, Chen MC, Hsu FN, Shazzad Hossain Prince GM, Chiu KY, Teng CJ, Yang TY, Wang HY, Yue CH, *et al*: Future aspects of CDK5 in prostate cancer: From pathogenesis to therapeutic implications. Int J Mol Sci 20: 3881, 2019.
2. Oner M, Chen MC, Cheng PT, Li YH, Cheng YC, Celik A, Soong SW, Hsu LW, Lin DY, Hossain Prince GMS, *et al*: Impact of metformin on neocortical development during pregnancy: Involvement of ERK and p35/CDK5 pathways. Chemosphere 358: 142124, 2024.
3. Oner M, Chen MC, Cheng PT and Lin H: Metformin inhibits nerve growth factor-induced sympathetic neuron differentiation through p35/CDK5 inhibition. Am J Physiol Cell Physiol 326: C1648-C1658, 2024.
4. Oner M, Cheng PT, Wang HY, Chen MC and Lin H: Metformin alters dendrite development and synaptic plasticity in rat cortical neurons. Biochem Biophys Res Commun 710: 149874, 2024.
5. Oner M, Lin E, Chiu KY, Chen MC, Prince GMSH, Lai CH, Hsieh JT, Wang HY and Lin HO: p35/CDK5 regulates bladder cancer proliferation and migration and promotes higher tumor grade and poor survival rate in patients with bladder cancer. Anticancer Res 44: 543-553, 2024.
6. Yue CH, Oner M, Chiu CY, Chen MC, Teng CL, Wang HY, Hsieh JT, Lai CH and Lin H: RET Regulates human medullary thyroid cancer cell proliferation through CDK5 and STAT3 activation. Biomolecules 11: 860, 2021.
7. Chen MC, Chen KC, Chang GC, Lin H, Wu CC, Kao WH, Teng CJ, Hsu SL and Yang TY: RAGE acts as an oncogenic role and promotes the metastasis of human lung cancer. Cell Death Dis 11: 265, 2020.
8. Chen MC, Huang CY, Hsu SL, Lin E, Ku CT, Lin H and Chen CM: Retinoic acid induces apoptosis of prostate cancer DU145 cells through cdk5 overactivation. Evid Based Complement Alternat Med 2012: 580736, 2012.
9. Hsu FN, Chen MC, Lin KC, Peng YT, Li PC, Lin E, Chiang MC, Hsieh JT and Lin H: Cyclin-dependent kinase 5 modulates STAT3 and androgen receptor activation through phosphorylation of Ser^{727} on STAT3 in prostate cancer cells. Am J Physiol Endocrinol Metab 305: E975-E986, 2013.
10. Kuo HS, Hsu FN, Chiang MC, You SC, Chen MC, Lo MJ and Lin H: The role of Cdk5 in retinoic acid-induced apoptosis of cervical cancer cell line. Chin J Physiol 52: 23-30, 2009.
11. Lin E, Chen MC, Huang CY, Hsu SL, Huang WJ, Lin MS, Wu JC and Lin H: All-trans retinoic acid induces DU145 cell cycle arrest through Cdk5 activation. Cell Physiol Biochem 33: 1620-1630, 2014.
12. Lin H, Chen MC, Chiu CY, Song YM and Lin SY: Cdk5 regulates STAT3 activation and cell proliferation in medullary thyroid carcinoma cells. J Biol Chem 282: 2776-2784, 2007.
13. Lin H, Chen MC and Ku CT: Cyclin-dependent kinase 5 regulates steroidogenic acute regulatory protein and androgen production in mouse Leydig cells. Endocrinology 150: 396-403, 2009.
14. Prince G, Yang TY, Lin H and Chen MC: Mechanistic insight of cyclin-dependent kinase 5 in modulating lung cancer growth. Chin J Physiol 62: 231-240, 2019.

15. Teng CJ, Cheng PT, Cheng YC, Tsai JR, Chen MC and Lin H: Dinaciclib inhibits the growth of acute myeloid leukemia cells through either cell cycle-related or ERK1/STAT3/MYC pathways. Toxicol In Vitro 96: 105768, 2024.
16. Karimian A, Ahmadi Y and Yousefi B: Multiple functions of p21 in cell cycle, apoptosis and transcriptional regulation after DNA damage. DNA Repair (Amst) 42: 63-71, 2016.
17. Foy R, Crozier L, Pareri AU, Valverde JM, Park BH, Ly T and Saurin AT: Oncogenic signals prime cancer cells for toxic cell overgrowth during a G1 cell cycle arrest. Mol Cell 83: 4047-4061. e6, 2023.
18. Dimri GP, Nakanishi M, Desprez PY, Smith JR and Campisi J: Inhibition of E2F activity by the cyclin-dependent protein kinase inhibitor p21 in cells expressing or lacking a functional retinoblastoma protein. Mol Cell Biol 16: 2987-2997, 1996.
19. Nakanishi M, Kaneko Y, Matsushime H and Ikeda K: Direct interaction of p21 cyclin-dependent kinase inhibitor with the retinoblastoma tumor suppressor protein. Biochem Biophys Res Commun 263: 35-40, 1999.
20. Hauge S, Macurek L and Syljuåsen RG: p21 limits S phase DNA damage caused by the Wee1 inhibitor MK1775. Cell Cycle 18: 834-847, 2019.
21. Pisonero-Vaquero S, Soldati C, Cesana M, Ballabio A and Medina DL: TFEB modulates p21/WAF1/CIP1 during the DNA damage response. Cells 9: 1186, 2020.
22. Huang PH, Chen MC, Peng YT, Kao WH, Chang CH, Wang YC, Lai CH, Hsieh JT, Wang JH, Lee YT, *et al*: Cdk5 directly targets nuclear p21CIP1 and promotes cancer cell growth. Cancer Res 76: 6888-6900, 2016.
23. Zhang Y, Zhang YJ, Zhao HY, Zhai QL, Zhang Y and Shen YF: The impact of R213 mutation on p53-mediated p21 activity. Biochimie 99: 215-218, 2014.
24. Chen DW, Lang BHH, McLeod DSA, Newbold K and Haymart MR: Thyroid cancer. Lancet 401: 1531-1544, 2023.
25. Sinha RA and Yen PM: Metabolic messengers: Thyroid hormones. Nat Metab 6: 639-650, 2024.
26. Basolo F, Macerola E, Poma AM and Torregrossa L: The 5th edition of WHO classification of tumors of endocrine organs: changes in the diagnosis of follicular-derived thyroid carcinoma. Endocrine 80: 470-476, 2023.
27. Modica R, Benevento E and Colao A: Endocrine-disrupting chemicals (EDCs) and cancer: New perspectives on an old relationship. J Endocrinol Invest 46: 667-677, 2023.
28. Ijaz K and Yin F: Papillary thyroid carcinoma with squamous dedifferentiation: A potential diagnostic pitfall. Anticancer Res 43: 255-258, 2023.
29. Ohashi R: Solid variant of papillary thyroid carcinoma: An under-recognized entity. Endocr J 67: 241-248, 2020.
30. Kang SY, Ahn HR, Youn HJ and Jung SH: Prognosis of papillary thyroid carcinoma in relation to preoperative subclinical hypothyroidism. Ann R Coll Surg Engl 103: 367-373, 2021.
31. Lee JS, Lee JS, Yun HJ, Kim SM, Chang H, Lee YS, Chang HS and Park CS: Aggressive subtypes of papillary thyroid carcinoma smaller than 1 cm. J Clin Endocrinol Metab 108: 1370-1375, 2023.
32. Mao J, Zhang Q, Zhang H, Zheng K, Wang R and Wang G: Risk factors for lymph node metastasis in papillary thyroid carcinoma: A systematic review and meta-analysis. Front Endocrinol (Lausanne) 11: 265, 2020.
33. Yu J, Deng Y, Liu T, Zhou J, Jia X, Xiao T, Zhou S, Li J, Guo Y, Wang Y, *et al*: Lymph node metastasis prediction of papillary thyroid carcinoma based on transfer learning radiomics. Nat Commun 11: 4807, 2020.
34. Zhang D, Zhu XL and Jiang J: Papillary thyroid carcinoma with breast and bone metastasis. Ear Nose Throat J 102: 259-262, 2023.
35. Daniels GH: Follicular thyroid carcinoma: A perspective. Thyroid 28: 1229-1242, 2018.
36. Pelizzo MR, Mazza EI, Mian C and Merante Boschin I: Medullary thyroid carcinoma. Expert Rev Anticancer Ther 23: 943-957, 2023.
37. Yang J and Barletta JA: Anaplastic thyroid carcinoma. Semin Diagn Pathol 37: 248-256, 2020.
38. Tjokorda Gde Dalem Pemayun: Current diagnosis and management of thyroid nodules. Acta Med Indones 48: 247-257, 2016.
39. Roman BR, Randolph GW and Kamani D: Conventional thyroidectomy in the treatment of primary thyroid cancer. Endocrinol Metab Clin North Am 48: 125-141, 2019.
40. Fullmer T, Cabanillas ME and Zafereo M: Novel therapeutics in radioactive iodine-resistant thyroid cancer. Front Endocrinol (Lausanne) 12: 720723, 2021.
41. Brierley JD: Update on external beam radiation therapy in thyroid cancer. J Clin Endocrinol Metab 96: 2289-2295, 2011.
42. Salvatore D, Santoro M and Schlumberger M: The importance of the RET gene in thyroid cancer and therapeutic implications. Nat Rev Endocrinol 17: 296-306, 2021.
43. Dong X, Akuetteh PDP, Song J, Ni C, Jin C, Li H, Jiang W, Si Y, Zhang X, Zhang Q and Huang G: Major vault protein (MVP) associated with BRAF ^{V600E} mutation is an immune microenvironment-related biomarker promoting the progression of papillary thyroid cancer via MAPK/ERK and PI3K/AKT pathways. Front Cell Dev Biol 9: 688370, 2022.
44. Nikiforov YE and Nikiforova MN: Molecular genetics and diagnosis of thyroid cancer. Nat Rev Endocrinol 7: 569-580, 2011.
45. Nozhat Z and Hedayati M: PI3K/AKT Pathway and its mediators in thyroid carcinomas. Mol Diagn Ther 20: 13-26, 2016.
46. Chou CK, Chi SY, Hung YY, Yang YC, Fu HC, Wang JH, Chen CC and Kang HY: Clinical impact of androgen receptor-suppressing miR-146b expression in papillary thyroid cancer aggressiveness. J Clin Endocrinol Metab 108: 2852-2861, 2023.
47. Livak KJ and Schmittgen TD: Analysis of relative gene expression data using real-time quantitative PCR and the 2(-Delta Delta C(T)) method. Methods 25: 402-408, 2001.
48. Cheng PT, Cheng YC, Oner M, Li YH, Chen MC, Wu JH, Chang TC, Celik A, Liu FL, Wang HY, *et al*: Antrodia salmonea extract inhibits cell proliferation through regulating cell cycle arrest and apoptosis in prostate cancer cell lines. Chin J Physiol 65: 209-214, 2022.
49. Chen CY, Li YH, Liao WL, Oner M, Cheng YC, Liu FL, Cheng PT, Celik A, Wu JH, Lai CH, *et al*: Antrodia salmonea extracts regulate p53-AR signaling and apoptosis in human prostate cancer LNCaP cells. Evid Based Complement Alternat Med 2022: 7033127, 2022.
50. Abramson J, Adler J, Dunger J, Evans R, Green T, Pritzel A, Ronneberger O, Willmore L, Ballard AJ, Bambrick J, *et al*: Accurate structure prediction of biomolecular interactions with AlphaFold 3. Nature 630: 493-500, 2024.
51. Lee YK, Rovira A, Carroll PV and Simo R: Management of aggressive variants of papillary thyroid cancer. Curr Opin Otolaryngol Head Neck Surg 32: 125-133, 2024.
52. Qu N, Chen D, Ma B, Zhang L, Wang Q, Wang Y, Wang H, Ni Z, Wang W, Liao T, *et al*: Integrated proteogenomic and metabolomic characterization of papillary thyroid cancer with different recurrence risks. Nat Commun 15: 3175, 2024.
53. Coca-Pelaz A, Shah JP, Hernandez-Prera JC, Ghossein RA, Rodrigo JP, Hartl DM, Olsen KD, Shaha AR, Zafereo M, Suarez C, *et al*: Papillary thyroid cancer-aggressive variants and impact on management: A narrative review. Adv Ther 37: 3112-3128, 2020.
54. Filetti S, Durante C, Hartl D, Leboulleux S, Locati LD, Newbold K, Papotti MG and Berruti A; ESMO Guidelines Committee. Electronic address: clinicalguidelines@esmo.org: Thyroid cancer: ESMO clinical practice guidelines for diagnosis, treatment and follow-up†. Ann Oncol 30: 1856-1883, 2019.
55. Gunabushanam G: Perfluorobutane-enhanced US helps differentiate benign lymph nodes from papillary thyroid cancer metastases. Radiology 307: e230581, 2023.
56. Schonfeld SJ, Morton LM, Berrington de Gonzalez A, Curtis RE and Kitahara CM: Risk of second primary papillary thyroid cancer among adult cancer survivors in the United States, 2000-2015. Cancer Epidemiol 64: 101664, 2020.
57. Gao GB, Sun Y, Fang RD, Wang Y, Wang Y and He QY: Post-translational modifications of CDK5 and their biological roles in cancer. Mol Biomed 2: 22, 2021.
58. Jin X, Yang C, Fan P, Xiao J, Zhang W, Zhan S, Liu T, Wang D and Wu H: CDK5/FBW7-dependent ubiquitination and degradation of EZH2 inhibits pancreatic cancer cell migration and invasion. J Biol Chem 292: 6269-6280, 2017.
59. Mandl MM, Zhang S, Ulrich M, Schmoeckel E, Mayr D, Vollmar AM and Liebl J: Inhibition of Cdk5 induces cell death of tumor-initiating cells. Br J Cancer 116: 912-922, 2017.
60. Liu C, Zhai X, Zhao B, Wang Y and Xu Z: Cyclin I-like (CCNI2) is a cyclin-dependent kinase 5 (CDK5) activator and is involved in cell cycle regulation. Sci Rep 7: 40979, 2017.
61. Zhang J, Li H and Herrup K: Cdk5 nuclear localization is p27-dependent in nerve cells: Implications for cell cycle suppression and caspase-3 activation. J Biol Chem 285: 14052-14061, 2010.
62. Bautista L, Knippler CM and Ringel MD: p21-activated kinases in thyroid cancer. Endocrinology 161: bqaa105, 2020.
63. Lu Z and Hunter T: Ubiquitylation and proteasomal degradation of the p21(Cip1), p27(Kip1) and p57(Kip2) CDK inhibitors. Cell Cycle 9: 2342-2352, 2010.

64. Takasugi T, Minegishi S, Asada A, Saito T, Kawahara H and Hisanaga S: Two degradation pathways of the p35 Cdk5 (cyclin-dependent kinase) activation subunit, dependent and independent of ubiquitination. J Biol Chem 291: 4649-4657, 2016.
65. Zhang S, Lu Z, Mao W, Ahmed AA, Yang H, Zhou J, Jennings N, Rodriguez-Aguayo C, Lopez-Berestein G, Miranda R, *et al*: CDK5 regulates paclitaxel sensitivity in ovarian cancer cells by modulating AKT activation, p21Cip1- and p27Kip1-mediated G1 cell cycle arrest and apoptosis. PLoS One 10: e0131833, 2015.
66. Havens CG and Walter JC: Mechanism of CRL4(Cdt2), a PCNA-dependent E3 ubiquitin ligase. Genes Dev 25: 1568-1582, 2011.
67. Jumper J, Evans R, Pritzel A, Green T, Figurnov M, Ronneberger O, Tunyasuvunakool K, Bates R, Žídek A, Potapenko A, *et al*: Highly accurate protein structure prediction with AlphaFold. Nature 596: 583-589, 2021.
68. Harper JW, Elledge SJ, Keyomarsi K, Dynlacht B, Tsai LH, Zhang P, Dobrowolski S, Bai C, Connell-Crowley L, Swindell E, *et al*: Inhibition of cyclin-dependent kinases by p21. Mol Biol Cell 6: 387-400, 1995.
69. Malumbres M: Cyclin-dependent kinases. Genome Biol 15: 122, 2014.
70. Hirai H, Kawanishi N and Iwasawa Y: Recent advances in the development of selective small molecule inhibitors for cyclin-dependent kinases. Curr Top Med Chem 5: 167-179, 2005.
71. Ardelt MA, Fröhlich T, Martini E, Müller M, Kanitz V, Atzberger C, Cantonati P, Meßner M, Posselt L, Lehr T, *et al*: Inhibition of cyclin-dependent kinase 5: A strategy to improve sorafenib response in hepatocellular carcinoma therapy. Hepatology 69: 376-393, 2019.
72. Lenjisa JL, Tadesse S, Khair NZ, Kumarasiri M, Yu M, Albrecht H, Milne R and Wang S: CDK5 in oncology: Recent advances and future prospects. Future Med Chem 9: 1939-1962, 2017.
73. Pozo K and Bibb JA: The emerging role of Cdk5 in cancer. Trends Cancer 2: 606-618, 2016.
74. Zhang M, Zhang L, Hei R, Li X, Cai H, Wu X, Zheng Q and Cai C: CDK inhibitors in cancer therapy, an overview of recent development. Am J Cancer Res 11: 1913-1935, 2021.